XIII ICSMFE, 1994, New Delhi, India / XIII CIMSTF, 1994, New Delhi, Inde

GENERAL STRESS-STRAIN-TIME EQUATION FOR SOILS

EQUATION GENERALE CONTRAINTE-DEFORMATION-TEMPS POUR LES SOLS

Eulalio Juarez-Badillo

Research Professor
Graduate School of Engineering,
National University of Mexico, Mexico

SYNOPSIS: The principle of Natural Proportionality is applied to find simple general equations to describe the strain-time relationship (creep) in the stable and in the unstable zones of the triaxial tests in soils. A general strength-time equation and a general K_o - time relationship are also given. The theoretical equations are applied to experimental data on drained and undrained triaxial tests already published in the literature.

INTRODUCTION

The principle of Natural Proportionality has been enunciated and applied to various physical phenomena (Juarez-Badillo, 1981, 1985a,b, 1990). This principle simply states that all physical phenomena are ordered and simple. The main problem is to find the proper variables from which the proper functions are defined and related through the proper non linear natural proportionality. This process is applied in this paper to obtain a general equation that relates deviatoric deformations to time (creep) in soils. The proper variable used to describe deviatoric deformation is the natural general shear deformation (Juárez-Badillo, 1974). Let x_1 (vertical), x_2 and x_3 be the Cartesian coordinate system and let us consider the simple case of a triaxial compression test, axial stress increased. The natural principal strains (Hencky) are defined by

$$\varepsilon_1 = \ln \frac{x_1}{x_{10}}, \quad \varepsilon_2 = \ln \frac{x_2}{x_{20}}, \quad \varepsilon_3 = \ln \frac{x_3}{x_{30}} \tag{1}$$

where x_{10}= initial x_1, where x_1 is the vertical dimension of the sample at time t, etc. In triaxial tests the following symbols are used: ε_a for the axial strain and ε_r for the radial strain. The natural volumetric strain is simply given by

$$\varepsilon_v = \ln \frac{V}{V_o} = \varepsilon_1 + \varepsilon_2 + \varepsilon_3 = \varepsilon_a + 2\varepsilon_r \tag{2}$$

where V_o= initial volume V. The isotropic component of strain ε is

$$\varepsilon = \frac{\varepsilon_1 + \varepsilon_2 + \varepsilon_3}{3} = \frac{\varepsilon_a + 2\,\varepsilon_r}{3} \tag{3}$$

and the deviatoric components of strain e_i are

$$e_1 = \varepsilon_1 - \varepsilon, \quad e_2 = \varepsilon_2 - \varepsilon, \quad e_3 = \varepsilon_3 - \varepsilon \tag{4}$$

or

$$e_a = \varepsilon_a - \varepsilon, \quad e_r = \varepsilon_r - \varepsilon \tag{5}$$

The natural general shear deformation η for our case is simply given by

$$\eta = e_1 - e_2 = \varepsilon_1 - \varepsilon_2 = \varepsilon_1 - \varepsilon_3 = e_1 - e_3 \tag{6}$$

Since from eqs. (3) an (5) we have that

$$e_a + 2\,e_r = 0 \tag{7}$$

then, from eqs. (6) and (7)

$$e_a = \frac{2}{3}\,\eta \tag{8}$$

STRAIN-TIME EQUATION

All triaxial tests on soils produce creep curves similar to the ones shown in Fig. 7 (Bishop, 1966). From these curves it is obvious that they all obey the principle of Natural Proportionality.

Let σ_{co} be the isotropic consolidation pressure in the first stage of the triaxial test and let $\Delta\sigma_a = \sigma_1 - \sigma_3$ be the axial increment of stress in the second stage of the test.

Some basic considerations of the problem are: when a certain value of $\sigma_1 - \sigma_3$ is applied, at t=0 we have e_a=0 and e_a increases to a final value e_{af} at t=∞ if the level of stress is below failure, that is, if we are in the stable zone. If the level of stress is in the unstable zone, failure will be produced and we will have e_a=∞ (the negative character of e_a is irrelevant at present) at a certain failure time t_f. The failure time t_f will be smaller as the level of stress increases. Between both zones, the stable zone and the unstable zone, there exists a certain threshold level of stress for which e_a=∞ at t=∞, the frontier failure curve.

Let us consider first the stable zone. If the axial deviatoric

strain e_a is a proper variable, its functional relation with time should be as follows. The variable time varies from 0 to ∞, it has a complete domain and, therefore, it is its proper function. The variable e_a varies from 0 to e_{af}, its domain is incomplete. Its proper function z, with a complete domain, is the simplest possible function, and it is

$$z = \frac{1}{e} - \frac{1}{e_f} \tag{9}$$

where, for simplicity, the subscript a has been dropped. Now we have that for t=0, z=∞ and for t=∞, z=0 . z has a complete domain and it is the proper function corresponding to the proper variable e. The proper proportionality between them is

$$\frac{dz}{z} = -\xi \frac{dt}{t} \tag{10}$$

where the minus sign takes into account that when t increases, z decreases and ξ is a constant of proportionality.

The constant ξ is a characteristic of the material (as it will be shown later) and it is a measure of the non linear shear viscosity of the material. A proper name for ξ is "shear fluidity", since ξ increases when the non linear viscosity decreases.

Integrating eq. (10) we obtain

$$\frac{z}{z_1} = \left(\frac{t}{t_1}\right)^{-\xi} \tag{11}$$

where (t_1,z_1) is a known point.

Introducing eq. (9) into eq. (11) we obtain

$$\frac{1}{e} - \frac{1}{e_f} = \left(\frac{1}{e_1} - \frac{1}{e_f}\right)\left(\frac{t}{t_1}\right)^{-\xi} \tag{12}$$

which may be written as

$$\frac{e_f}{e} = 1 + \left(\frac{e_f}{e_1} - 1\right)\left(\frac{t}{t_1}\right)^{-\xi} \tag{13}$$

An elegant and simple way of writing eq. (13) is in terms of the point for which $e_1 = 0.5e_f$ at $t_1=t^*$ where t^* is the "characteristic time". Then, eq. (13) may be written as:

$$e = \frac{e_f}{1+\left(\frac{t}{t^*}\right)^{-\xi}} \tag{14}$$

However, a useful equation in practice is eq. (13) in the form:

$$\frac{e}{e_1} = \frac{\frac{e_f}{e_1}}{1+\left(\frac{e_f}{e_1}-1\right)\left(\frac{t}{t_1}\right)^{-\xi}} \tag{15}$$

For the frontier failure curve, when $e_f=\infty$ for t=∞, from eq. (12) we obtain

$$\frac{e}{e_1} = \left(\frac{t}{t_1}\right)^{\xi} \tag{16}$$

Let us now consider the unstable zone. Now e has a complete domain from 0 to ∞ , while t varies from 0 to t_f. Proceeding in a very similar way we now have that the proper function for t is

$$z = \frac{1}{t} - \frac{1}{t_f} \tag{17}$$

Now we have that for e=0, z=∞ and for e=∞, z=0. The proper proportionality between them is now

$$\frac{de}{e} = -\xi \frac{dz}{z} \tag{18}$$

where the constant of proportionality ξ is assumed to be the same than for the stable zone since it is a measure of the fluidity of the material.

Integrating eq. (18) we obtain

$$\frac{e}{e_1} = \left(\frac{z}{z_1}\right)^{-\xi} \tag{19}$$

Introducing eq. (17) into eq. (19) we obtain

$$\frac{e}{e_1} = \left(\frac{\frac{1}{t} - \frac{1}{t_f}}{\frac{1}{t_1} - \frac{1}{t_f}}\right)^{-\xi} \tag{20}$$

which may be written as

$$\frac{e}{e_1} = \left(\frac{\frac{t_f}{t} - 1}{\frac{t_f}{t_1} - 1}\right)^{-\xi} \tag{21}$$

An elegant and simple way of writing eq. (21) is in terms of the point for which $t_1=0.5t_f$ at $e_1=e^*$ where e^* is the "characteristic e". Then eq. (21) may be written as

$$e = e^* \left(\frac{t_f}{t} - 1\right)^{-\xi} \tag{22}$$

For the frontier failure curve, when $e_f=\infty$ for $t_f=\infty$, from eq. (20) we again obtain eq. (16).

In the unstable zone the rate of strain, from eq. (21), is

$$\dot{e} = \frac{de}{dt} = \xi \frac{1}{1 - \frac{t}{t_f}} \frac{e}{t} \tag{23}$$

It may be observed that for the frontier failure curve, eqs. (16) or (23) provide

$$\dot{e} = \xi \frac{e}{t} \tag{24}$$

That is, for the frontier failure curve, the instantaneous rate of deformation is ξ times the mean rate of deformation.

For the failure curves one important point is when the rate of strain changes from decreasing to increasing, that is when $\frac{d\dot{e}}{dt} = 0$. It t' is the time at which this occurs, from eq. (23) it may be found that

$$t' = \frac{1-\xi}{2} t_f \tag{25}$$

that is, the change occurs at a time t' somewhat smaller than half the failure time t_f.

The minimum value of $\dot{e}$, that is, the value of $\dot{e}$ at t=t' is, from eq. (23)

$$(\dot{e})_{min} = 2\,\frac{\xi}{1+\xi}\,\frac{e}{t'} = 4\,\frac{\xi}{(1+\xi)(1-\xi)}\,\frac{e}{t_f} \qquad (26)$$

Fig. 1 presents the graphs of the creep curves in log-log plot for different values of ξ, eq. (15) for the stable zone, eq. (16) for the frontier failure curves and eq. (21) for the unstable zone. All curves are plotted using for the stable curves $e_f = 10\ e_1$ and for the failure curves $t_f = 100\ t_1$. Important characteristics of them are noted in the figure. All frontier failure curves are straight lines where ξ are the slopes. All stable curves plot below the frontier failure curves and are concave downwards. All failure curves plot above the frontier failure curves and are concave upwards. The characteristic times have been noted in the stable curves as well as their middle thirds that plot very close to straight lines in semi-log plot. The characteristic strains and the points where $\frac{de}{dt} = 0$ have been noted in the failure curves.

Fig. 2 presents the graphs of the same equations in semi-log plots. All stable curves are symmetric with respect to their middle points; they are concave upwards in their first half and concave downwards in their second half; their middle third is very close to a straight line. Further properties of these stable curves may be seen in (Juarez-Badillo, 1985a) since their equations are of the same structure than the general equation of secondary compression for soils. All frontier failure curves and failures curves are concave upwards.

The characteristic of the stable curves whose middle third is practically a straight line is very useful in practice. This property allows to estimate e_f. Note also that in failure curves, and depending on the value of ξ, their separation from the frontier failure curves occur somewhat "late", let us say, one cycle before t_f. This, for low values of ξ, allows in practice to estimate ξ from the beginning of the failure curves and later on permits the calculation of t_f from the last part of the experimental creep curves.

Fig. 3 shows the graphs of failure curves, eq. (22), for various values of ξ.

In practice it might be useful the log-log plots of the strain rates. For the stable zone, from eq. (14) it is obtained

$$\dot{e} = \xi\,\frac{e_f}{t^*}\left(\frac{t}{t^*}\right)^{-1-\xi}\left[1+\left(\frac{t}{t^*}\right)^{-\xi}\right]^{-2} \qquad (27)$$

At time $t=t^*$ we simply get

$$\dot{e}_{t=t^*} = \frac{1}{4}\,\xi\,\frac{e_f}{t^*} \qquad (28)$$

Normalyzing eq. (27) by eq. (28) we get

$$\frac{\dot{e}}{\dot{e}_{t=t^*}} = 4\,\xi\left(\frac{t}{t^*}\right)^{-1-\xi}\left[1+\left(\frac{t}{t^*}\right)^{-\xi}\right]^{-2} \qquad (29)$$

One important characteristic is the slope in log-log plot. From eq. (27) it is obtained

$$\frac{d\,\log\,\dot{e}}{d\,\log\,t} = -(1+\xi) + \frac{2\,\xi}{1+\left(\frac{t}{t^*}\right)^{\xi}} \qquad (30)$$

From eq. (30) we see that the slope decreases from $-(1-\xi)$ at

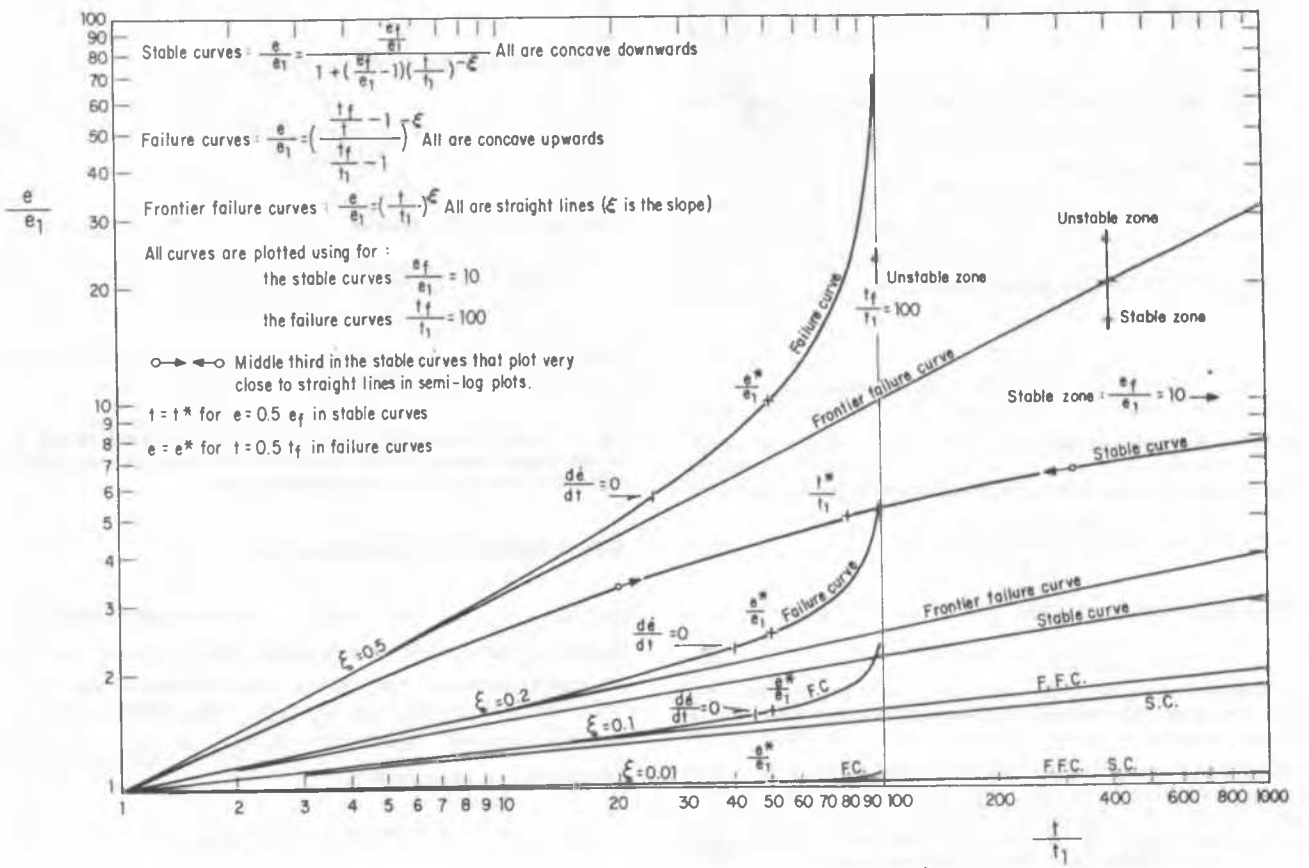

Fig 1 Graphs of creep curves for different values of ξ

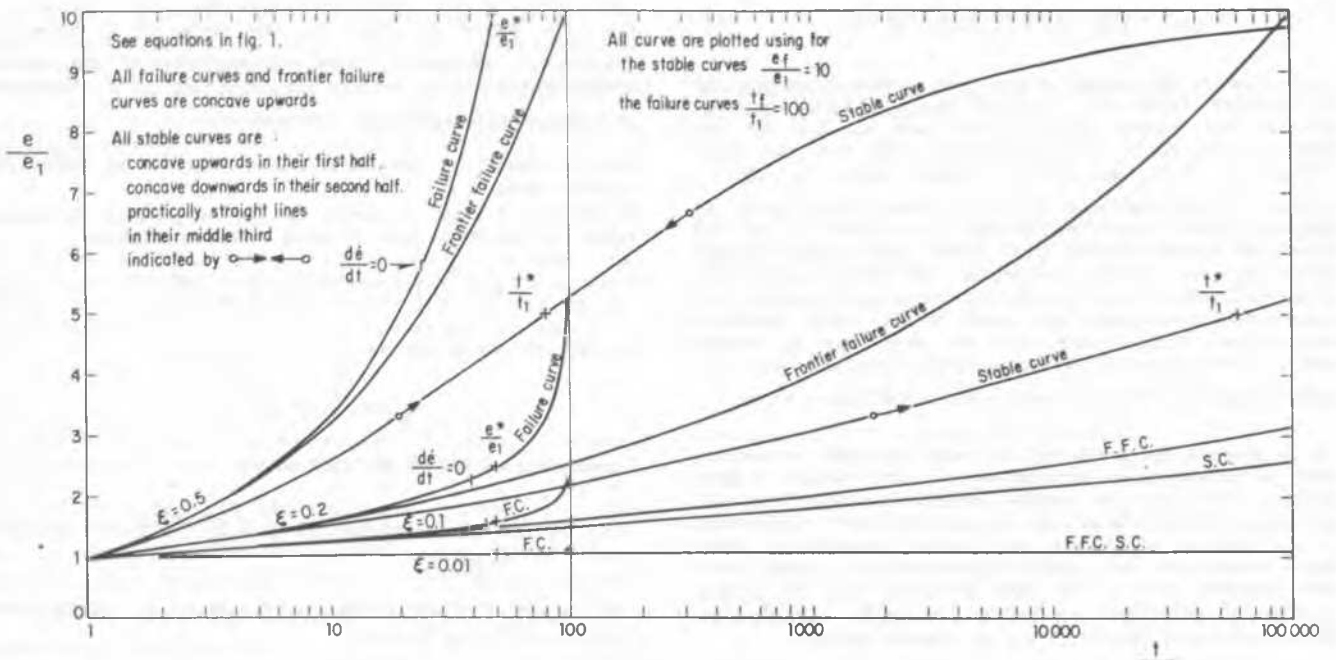

Fig. 2. Graphs of creep curves for different values of ξ

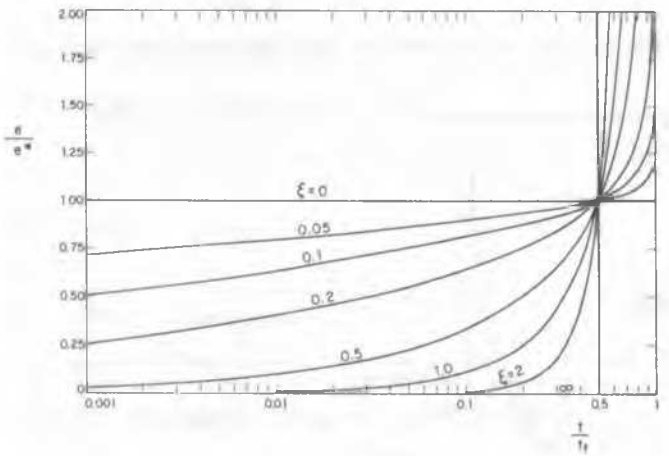

Fig. 3. Graphs of $\frac{e}{e^*}=\left(\frac{t_f}{t}-1\right)^{\xi}$ for various values of ξ

$t = 0$ to $-(1+\xi)$ at $t = \infty$ (See Fig. 4).

For the frontier failure curve, from eq. (16) we get

$$\dot{e} = \xi \frac{e_1}{t_1}\left(\frac{t}{t_1}\right)^{\xi-1} \tag{31}$$

From this eq. (31) it is obtained

$$\frac{d \log \dot{e}}{d \log t} = -(1-\xi) \tag{32}$$

that is, the slope is constant all the way through, from $t = 0$ to $t = \infty$.

For the unstable zone, from eq. (22) it is obtained

$$\dot{e} = \xi \frac{e^*}{t_f}\frac{\frac{t_f}{t}}{1-\frac{t}{t_f}}\left(\frac{t_f}{t}-1\right)^{-\xi} \tag{33}$$

At $t = \frac{t_f}{2}$ we simply get

$$\dot{e}^* = 4\,\xi\,\frac{e^*}{t_f} \tag{34}$$

Normalyzing eq. (33) by eq. (34) we get

$$\frac{\dot{e}}{\dot{e}^*} = \frac{1}{4}\frac{\frac{t_f}{t}}{1-\frac{t}{t_f}}\left(\frac{t_f}{t}-1\right)^{-\xi} \tag{35}$$

From eq. (33) it is obtained

$$\frac{d \log \dot{e}}{d \log t} = -2 + \frac{1+\xi}{1-\frac{t}{t_f}} \tag{36}$$

From eq. (36) me see that the slope increases from $-(1-\xi)$ at $t = 0$ to ∞ at $t = t_f$ (See Fig. 5).

Fig. 4 shows the graphs of eq. (29) for different values of ξ in the stable zone and Fig. 5 shows the graphs of eq. (35) for different values of ξ in the unstable zone.

SHEAR STRENGTH–TIME EQUATION

Let $(\sigma_1-\sigma_3)_{f\infty}$ be the level of stress that produces the frontier failure curve with failure time $t_f = \infty$. If the level of stress increases the failure time decreases and, at the limit, we have $(\sigma_1-\sigma_3)_f = \infty$ for $t_f = 0$. The domain for t_f is complete but the domain for $(\sigma_1-\sigma_3)_f$ is not. The proper function for $(\sigma_1-\sigma_3)_f$ is now

$$z = (\sigma_1-\sigma_3)_f - (\sigma_1-\sigma_3)_{f\infty} \tag{37}$$

Now, for $t_f = 0$, $z = \infty$ and for $t_f = \infty$, $z = 0$. The relationship

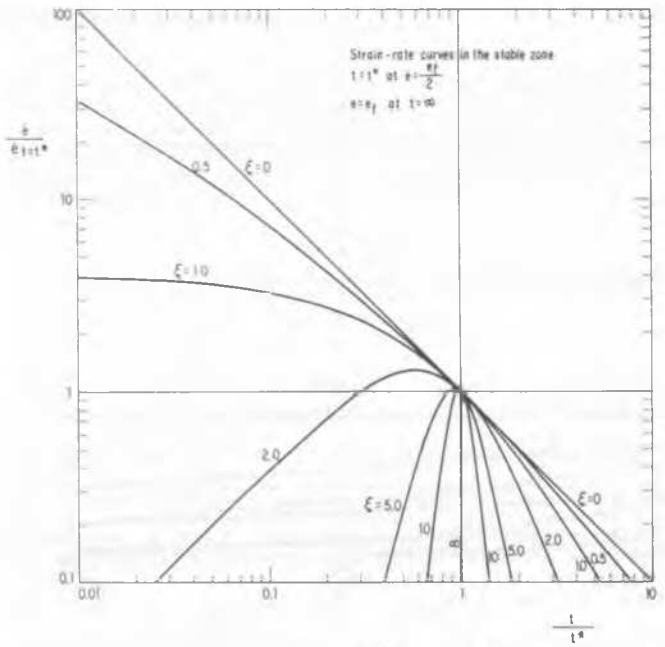

Fig 4 Graphs of $\frac{\dot{e}}{\dot{e}_{t=t^*}} = 4\left(\frac{1}{t^*}\right)^{1-\xi}\left[1+\left(\frac{1}{t^*}\right)^{\xi}\right]^{-2}$

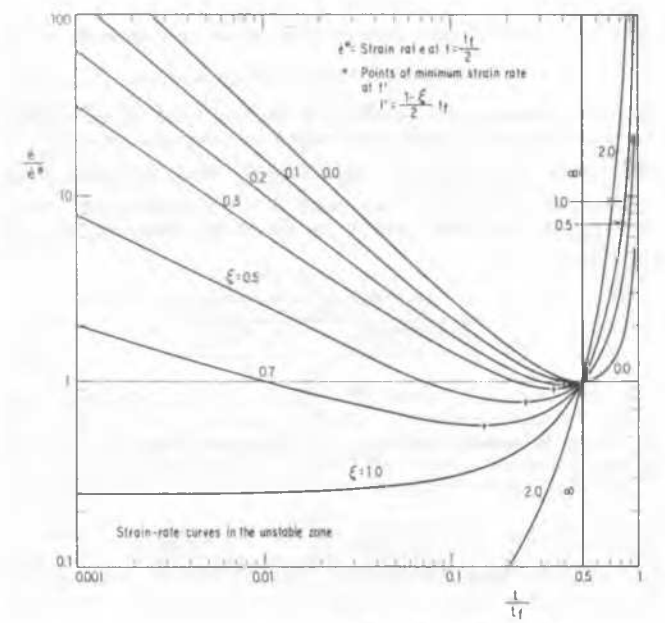

Fig. 5. Graphs of $\frac{\dot{e}}{\dot{e}^*} = \frac{1}{4}\,\frac{\frac{t_f}{t}}{1-\frac{t}{t_f}}\left(\frac{t_f}{t}-1\right)^{-\xi}$

betwen them should be

$$\frac{dz}{z} = -\zeta\,\frac{dt}{t} \tag{38}$$

where ζ is the "strength fluidity" of the material.

Integrating eq. (38) we obtain

$$\frac{z}{z_1} = \left(\frac{t}{t_1}\right)^{-\zeta} \tag{39}$$

Introducing eq. (37) into eq. (39) we obtain

$$\frac{(\sigma_1-\sigma_3)_f - (\sigma_1-\sigma_3)_{f\infty}}{(\sigma_1-\sigma_3)_{f1} - (\sigma_1-\sigma_3)_{f\infty}} = \left(\frac{t}{t_1}\right)^{-\zeta} \tag{40}$$

which may be written as

$$\frac{(\sigma_1-\sigma_3)_f}{(\sigma_1-\sigma_3)_{f\infty}} = 1+\left[\frac{(\sigma_1-\sigma_3)_{f1}}{(\sigma_1-\sigma_3)_{f\infty}} -1\right]\left(\frac{t}{t_1}\right)^{-\zeta} \tag{41}$$

Again, if it is chosen as the known point the point for which $(\sigma_1-\sigma_3)_{f1} = 2\,(\sigma_1-\sigma_3)_{f\infty}$ at the characteristic time $t_1 = t^*$, then eq. (41) may be written as

$$\frac{(\sigma_1-\sigma_3)_f}{(\sigma_1-\sigma_3)_{f\infty}} = 1 + \left(\frac{t}{t^*}\right)^{-\zeta} \tag{42}$$

where, for simplicity, the subscript f for t has been dropped in the above analysis.

If $(\sigma_1-\sigma_3)_{f\infty} = 0$ the resulting equation is obvious from eq.(40).

Fig. 6 presents graphs of eq. (42) for various values of ζ.

OBTENTION OF PARAMETERS

The structure of the above equations for the relationship of strain and strength with time is the same than for the "general compressibility equation for soils" (Juarez-Badillo, 1981) and for the "general time volume change equation for soils" (Juarez-Badillo, 1985a). Further properties of these equations are treated in detail in these references. In the present paper some brief indications for the determination of parameters are given.

The semilog plot is the best plot for the stable creep curves. If the experimental curves allow to determine the beginning of the straight section at e=a, then $e_f = 3a$. If not, a trial and error procedure is needed. Three points in the experimental curve are needed: an early point 3, a middle point 1 and a final point 2. Then the value of ξ can be calculated from points 1 and 2 and eq. (13) in the form:

$$\xi = \frac{\log \dfrac{e_2}{e_1}\,\dfrac{e_f-e_1}{e_f-e_2}}{\log \dfrac{t_2}{t_1}} \tag{43}$$

Later on, using point 3 the values of e_f and ξ are confirmed using eq. (13). Generally a second and a third trial are needed until point 3 checks. Later on the characteristic time is calculated using eq. (14) in the form:

$$t^* = t_2\left(\frac{e_f - e_2}{c_2}\right)^{1/\xi} \tag{44}$$

Once e_f, ξ and t^* are known, these values are entered in eq. (14).

The log-log plot is the best plot for the failure creep curves. However, with some experience, the semi-log plot Is such as good. If t_f is not known, it may be guessed and a very similar procedure than for the stable creep curves may be followed. However an alternative and more convenient procedure in practice is: first to check the value of ξ (from the stable creep curves) with the first part of the experimental curves; if $\xi < 0.2$, the first part should be considered at least one cycle before failure, see Figs. 1 and 2; using eq. (16) in the

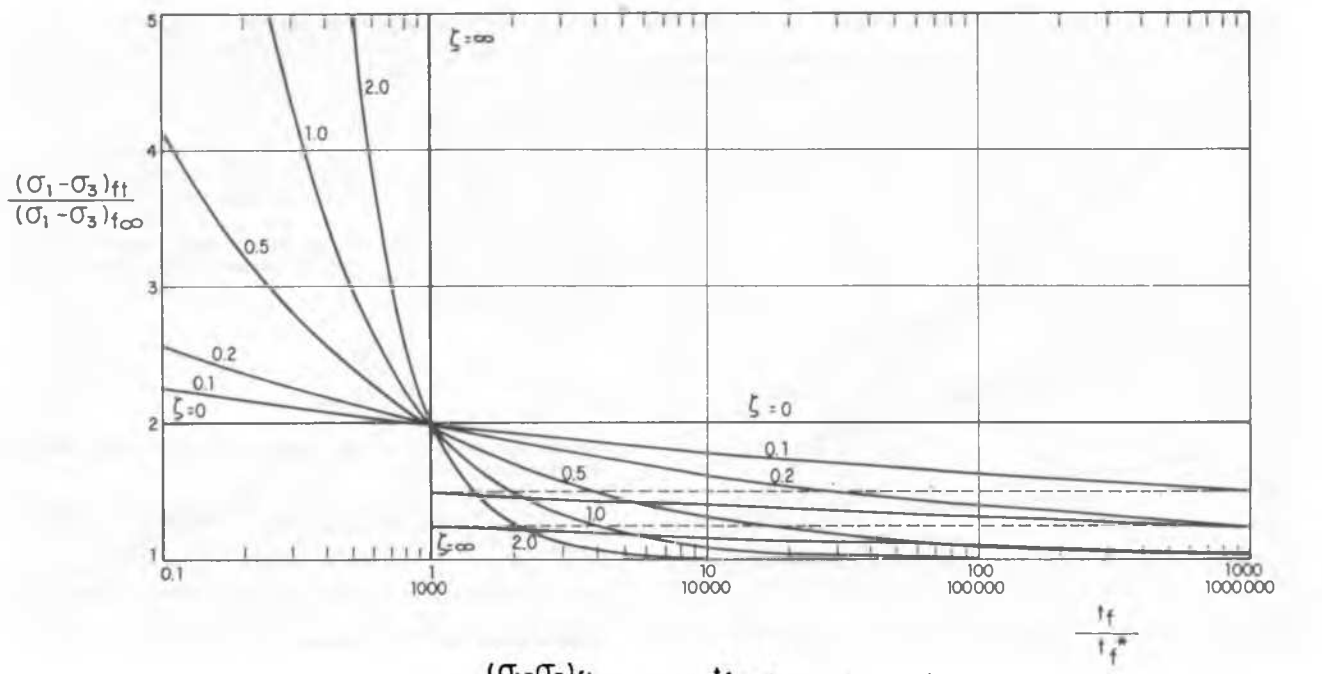

Fig. 6 Graphs of $\frac{(\sigma_1-\sigma_3)_{ft}}{(\sigma_1-\sigma_3)_{f\infty}} = 1 + (\frac{t_f}{t_f^*})^{\zeta}$ for various ζ.

form:

$$\xi = \frac{\log \frac{e_2}{e_1}}{\log \frac{t_2}{t_1}} \tag{45}$$

Later on with a final point 3, the failure time t_f may be calculated from eq. (21) in the form:

$$t_f = t_3 \frac{\left(\frac{e_3}{e_1}\right)^{1/\xi} - 1}{\left(\frac{e_3}{e_1}\right)^{1/\xi} - \frac{t_3}{t_1}} \tag{46}$$

If the rate of strain $\dot{e}$ is known at point 3, t_f may be calculated from eq. (23) in the form:

$$t_f = \frac{t}{1 - \frac{\xi e}{\dot{t}e}} \tag{47}$$

Equation (47) is valid for the whole curve, but the aproximation is better for points closer to t_f.

If t_f is known, a useful equation for ξ, from eq. (21), is:

$$\xi = \frac{\log \frac{e_3}{e_1}}{\log \frac{t_3}{t_1} \frac{t_f - t_1}{t_f - t_3}} \tag{48}$$

The value of e^* is then calculated from eq. (22) in the form:

$$e^* = e_3 \left(\frac{t_f}{t_3} - 1\right)^{\xi} \tag{49}$$

Once t_f, ξ and e^* are known, these values are entered in eq. (22).

For the strength-time equation, a semi-log plot is very good. Three experimental points are needed to determine $(\sigma_1-\sigma_3)_{f\infty}$, ζ and t_f^*: an early point 1, say, at (0.1-1 min), a middle point 2 (10 - 100 min) and a late point 3 (1,000-10,000 min). First $(\sigma_1-\sigma_3)_{f\infty}$ is estimated and ζ is calculated from eq. (41) in the form:

$$\zeta = \frac{\log \frac{(\sigma_1-\sigma_3)_{f2} - (\sigma_1-\sigma_3)_{f\infty}}{(\sigma_1-\sigma_3)_{f3} - (\sigma_1-\sigma_3)_{f\infty}}}{\log \frac{t_3}{t_2}} \tag{50}$$

or, if ζ is known, $(\sigma_1-\sigma_3)_{f\infty}$ is calculated from eq. (41) in the form:

$$(\sigma_1-\sigma_3)_{f\infty} = \frac{(\sigma_1-\sigma_3)_{f3}(\frac{t_3}{t_2})^{\zeta} - (\sigma_1-\sigma_3)_{f2}}{(\frac{t_3}{t_2})^{\zeta} - 1} \tag{51}$$

Later on the values of $(\sigma_1-\sigma_3)_{f\infty}$ and ζ are confirmed using eq. (41) and point 1. The values of $(\sigma_1-\sigma_3)_{f\infty}$ and ζ should be modified until point 1 checks. Finally the characteristic failure time t_f^* is calculated from eq. (42) in the form:

$$t^* = t_1 \left[\frac{(\sigma_1-\sigma_3)_{f1} - (\sigma_1-\sigma_3)_{f\infty}}{(\sigma_1-\sigma_3)_{f\infty}}\right]^{\frac{1}{\zeta}} \tag{52}$$

Once $(\sigma_1-\sigma_3)_{f\infty}$, ζ and t_f^* are known, these values are entered in eq. (42).

STRESS-STRAIN EQUATION

"Basic stress strain equation for clays" (Juarez-Badillo, 1988) is the title of a paper pending of publication where a stress-strain equation is postulated and applied to Weald clay. Taking that paper as a basis the following equation is considered in this paper for the practical application that will be made:

$$de_a = -\frac{1}{3}\,\mu\,\frac{\sigma_{co}}{\sigma_{eo}}\,\frac{\dfrac{d(\sigma_1-\sigma_3)}{\sigma_{co}}}{\left[1-\dfrac{\sigma_1-\sigma_3}{(\sigma_1-\sigma_3)_f}\right]^{\nu}} \tag{53}$$

where μ and ν are two constant parameters called the coefficient of shear deformation and the shear exponent respectively and $\frac{\sigma_{eo}}{\sigma_{co}}$ is the overconsolidation factor where σ_{eo} is the equivalent consolidation pressure, that is, the pressure on the virgin compression curve corresponding to the void ratio of the sample. The overconsolidation factor can be found from the overconsolidation ratio $\frac{\sigma_p}{\sigma_{co}}$ by the equation (Juarez-Badillo, 1975), (Juarez-Badillo and Rico-Rodriguez, 1975).

$$\frac{\sigma_{eo}}{\sigma_{co}} = \left(\frac{\sigma_p}{\sigma_{co}}\right)^{1-\rho} \tag{54}$$

where ρ is the expansibility-compressibility ratio.
Integration of eq. (53) gives, for $\nu = 1$

$$e_a = \frac{1}{3}\,\mu\,\frac{\sigma_{co}}{\sigma_{eo}}\left(\frac{\sigma_1-\sigma_3}{\sigma_{co}}\right)_f \ln\left[1-\frac{\sigma_1-\sigma_3}{(\sigma_1-\sigma_3)_f}\right] \tag{55}$$

and for $\nu = 2$

$$e_a = -\frac{1}{3}\,\mu\,\frac{\sigma_{co}}{\sigma_{eo}}\left(\frac{\sigma_1-\sigma_3}{\sigma_{co}}\right)_f \left[\frac{1}{1-\dfrac{\sigma_1-\sigma_3}{(\sigma_1-\sigma_3)_f}}-1\right] \tag{56}$$

The experience of the author with Weald clay indicates that eq. (55), $\nu = 1$, is very good for drained tests while eq. (56), $\nu = 2$, is fairly good for undrained tests. However, at high overconconsolidation ratios, for some undrained tests, the coefficient μ seems to increase very much in eq. (56).

It should be observed that eq. (56) is very similar to the hyperbolic stress-strain response proposed by (Kondner, 1963) for cohesive soils. The main differences being that in eq. (56) e_a is the natural deviatoric axial strain instead of the common total axial strain in Kondner's equation and that the constants considered in eq. (56) for the hyperbolic function are introduced. Eq. (55) may also be referred to as the logarithmic stress-strain response.

STRESS-STRAIN-TIME EQUATION

Stress-strain equations (55) and (56) do not consider the variation of the strain with time. They refer to the "instantaneous" strain when stress is applied, say for $t = 1$ min for undrained tests and $t = t_p$ for drained tests where t_p is the time for primary compression. But in reality $e_a = 0$ for $t = 0$ and $e_a = e_f$ for $t = \infty$. If we make the hypotesis that in eqs. (55) and (56) the coefficient μ is a function of time and that all other quantities are time independent, we can write, from eqs. (14), (55) and (56):

$$\mu = \frac{\mu_\infty}{1+\left(\frac{t}{t^*}\right)^{-\xi}} \tag{57}$$

A further application to be studied in the future, is to consider the variation of $(\sigma_1-\sigma_3)_f$ with time, writing from eq. (42)

$$(\sigma_1-\sigma_3)_f = (\sigma_1-\sigma_3)_{f\infty}\left[1+\left(\frac{t}{t^*}\right)^{-\zeta}\right] \tag{58}$$

For the present paper, we can write, from eqs. (55), (56) and (57)

For drained tests, $\nu = 1$

$$e_a = \frac{1}{3}\,\mu_\infty\,\frac{\sigma_{co}}{\sigma_{eo}}\left(\frac{\sigma_1-\sigma_3}{\sigma_{co}}\right)_f \ln\left[1-\frac{\sigma_1-\sigma_3}{(\sigma_1-\sigma_3)_f}\right]\frac{1}{1+\left(\frac{t}{t^*}\right)^{-\xi}} \tag{59}$$

For undrained tests, $\nu = 2$

$$e_a = -\frac{1}{3}\,\mu_\infty\,\frac{\sigma_{co}}{\sigma_{eo}}\left(\frac{\sigma_1-\sigma_3}{\sigma_{co}}\right)_f\left[\frac{1}{1-\dfrac{\sigma_1-\sigma_3}{(\sigma_1-\sigma_3)_f}}-1\right]\frac{1}{1+\left(\frac{t}{t^*}\right)^{-\xi}} \tag{60}$$

K_o-TIME EQUATION

In the unpublished mentioned paper "Basic stress-strain equation for clays", for $\nu = 1$, the following equation for K_o was found:

$$K_o = \frac{\dfrac{1}{\sin\phi}+\dfrac{\mu}{\gamma}-1}{\dfrac{1}{\sin\phi}+\dfrac{\mu}{\gamma}+1} \tag{61}$$

where K_o is the earth coefficient at rest, ϕ = angle of internal friction and γ = coefficient of compresibility in the equation (Juarez-Badillo, 1975).

$$\frac{V}{V_1} = \left(\frac{\sigma}{\sigma_1}\right)^{-\gamma} \tag{62}$$

where V = Volume and (σ_1, V_1) is a known point.

Assuming again that sin ϕ is time independent, we have that K_o is time dependent because μ is a function of time, eq. (57). The coefficient of compressibility γ is time independent.

Some data on the variation of K_o with time appears in (Mesri and Castro, 1987). These data appear as values of $\frac{\Delta K_o}{\Delta \log t}$. Differentiating eq. (61) we may obtain:

$$\frac{dK_o}{d\log t} = 4.6\,\frac{\mu_\infty}{\gamma}\,\frac{\xi}{\left[1+\left(\frac{t^*}{t}\right)^{\xi}\right]^2}\left(\frac{t^*}{t}\right)^{\xi} \cdot \frac{1}{\left[\dfrac{1}{\sin\phi}+1+\dfrac{\mu_\infty}{\gamma}\,\dfrac{1}{1+\left(\frac{t^*}{t}\right)^{\xi}}\right]^2} \tag{63}$$

For $t = t^*$ eq. (63) becomes:

$$\left[\frac{dK_o}{d\log t}\right]_{t=t^*} = 1.15\,\frac{\mu_\infty}{\gamma}\,\frac{\xi}{\left[\frac{1}{\sin\phi} + 1 + \frac{1}{2}\frac{\mu_\infty}{\gamma}\right]^2} \qquad (64)$$

Direct calculation of eq. (63) shows that the maximum values of $\frac{dK_o}{d\log t}$ are of the order of 25% higher than the values given by eq. (64) and that they occur at times various orders of magnitud smaller than t^*.

PRACTICAL APPLICATION

Practical application of the above theory was made using experimental data contained in (Singh and Mitchell, 1968). These data show the variation of the common total axial strain ε_c (Cauchy) with time in compression triaxial tests, increasing the axial stress. The relationship of the natural deviatoric axial strain e_a to the common axial strain ε_c is:

$$e_a = \varepsilon_a - \frac{\varepsilon_v}{3} = \ln\frac{x_1}{x_{10}} - \frac{\varepsilon_v}{3} = \ln\left(1 + \frac{\Delta x_1}{x_{10}}\right) - \frac{\varepsilon_v}{3}$$

$$\therefore\ e_a = \ln(1 + \varepsilon_c) - \frac{\varepsilon_v}{3} \qquad (65)$$

In undrained tests, the isotropic component $\frac{\varepsilon_v}{3} = 0$ and in drained tests the isotropic component is, normally, very small compared to the natural axial strain, except in normally consolidated samples of very compressible clays. Therefore, the isotropic component was ignored. Furthermore, most of the experimental data show maximum values of $\varepsilon_c = -5\%$ to which a value of $e_a = -5.13\%$. corresponds. Therefore, for simplicity, they were considered equivalent. So it was assumed that

$$e_a = \varepsilon_c \qquad (66)$$

Furthermore, in this first analysis of experimental data, the variation of strength with time was also ignored as already mentioned.

All experimental data were analyzed following the procedure described in Obtention of parameters. First the creep parameters e_f, ξ and t^*, eq. (14), were obtained from the stable curves, with slight adjustments to e_f to conform to one of the stress strain equations (55) or (56) to arrive to a final eq. (59), $\nu = 1$, for the drained tests and eq. (60), $\nu = 2$, for the undrained tests. The values found for the different quantities are given in the figures and here the final equations will be presented. For the failure curves the procedure was similar, finding first the creep parameters t_f, ξ and e^*, eq. (22). The final equations are also given in this section.

Figs. 7 and 8 show drained creep tests on undisturbed brown London clay from Hendon. With the data shown in Fig. 7 the final equations are, for the stable curves, eq. (59), $\nu = 1$

$$e_a,\% = 5.0\,\ln\left[1 - \frac{\sigma_1-\sigma_3}{(\sigma_1-\sigma_3)_f}\right]\frac{1}{1+\left(\frac{t}{10^9}\right)^{-0.045}} \qquad (67)$$

and, for the failure curve, eq. (22)

$$-e_a,\% = 3.55\left(\frac{3{,}120}{t} - 1\right)^{-0.055} \qquad (68)$$

In these figures "the applied principal stress differences are percentages of the peak values measured in drained triaxial tests of 5 days duration". The fixed percentages shown were the values used in eq. (67).

Here it was found $\xi = 0.045$ for the stable curves and $\xi = 0.055$ for the failure curve. In Fig. 8 it should be observed that the experimental points at t = 10 min, specially the point with stress level 90-106%, which failed at t = 3,120 min = 2 days 4 hrs., indicate a greater strength at t = 10 min, of the order of 10%, than at t = 300,000 min = 208 days.

In practice an important quantity is the fraction of the "instantaneous strain" at $t = t_p$ or, say, t = 10 min, with respect to the total strain at $t = \infty$. This can be calculated from eqs. (14) and (57). Then, we can write, for the stable curves

$$\xi = 0.045,\ t^* = 10^9 \text{ min},\ \frac{e_{10}}{e_\infty} = \frac{\mu_{10}}{\mu_\infty} = 0.30 \qquad (69)$$

Figs. 9 and 10 show undrained creep tests on overconsolidated indisturbed San Francisco Bay mud. With the data shown in Fig. 9 the final equations are, for the stable curves, eq. (60), $\nu = 2$

$$-e_a,\% = 3.5\left[\frac{1}{1-\frac{\sigma_1-\sigma_3}{1.2}} - 1\right]\frac{1}{1+\left(\frac{t}{75{,}000}\right)^{-0.18}} \qquad (70)$$

and, for the failure curve, eq. (22)

$$-e_a,\% = 6.15\left(\frac{3{,}300}{t} - 1\right)^{-0.20} \qquad (71)$$

Here it was found $\xi = 0.18$ for the stable curves and $\xi = 0.20$ for the failure curve. In Fig. 10 it should be observed that the experimental points appear to indicate higher strength at t= 1 min than at t = 1,000 min . In this case the upper curve, D= 0.99 kg/cm^2, was found to be a failure curve. A probable frontier failure curve has been plotted, eq. (16), using $\xi = 0.18$ and $-e_1 = 1.1\%$ for $t_1 = 1$ min.

For these undrained tests, if we consider the "instantaneous strain" at t = 1 min, we can write for the stable curves, from eqs. (14) and (57):

$$\xi = 0.18,\ t^* = 75{,}000 \text{ min},\ \frac{e_1}{e_\infty} = \frac{\mu_1}{\mu_\infty} = 0.12 \qquad (72)$$

Fig. 11 shows drained creep tests on two samples of dry illite. Taking the geometrical average of the data shown in Fig. 11 we can write for them the final equation as, eq. (14):

$$-e_a,\% = \frac{2.8}{1+\left(\frac{t}{2.4\times10^9}\right)^{-0.062}} \qquad (73)$$

Considering the "instantaneous strain" at t = 1 min we can write for this case:

$$\xi = 0.062,\ t^* = 2.4\times10^9 \text{ min},\ \frac{e_1}{e_\infty} = \frac{\mu_1}{\mu_\infty} = 0.21 \qquad (74)$$

Figs. 12 and 13 show undrained creep of saturated remolded illite. "Water content of all samples = 34.3 $\pm$0.1%. All samples initially consolidated to $\sigma'_c = 2.0$ kg/cm^2 at 68°F, then overconsolidated by increasing Temp. to 110°F under undrained conditions. Cell pressure = 4.0 kg/cm^2". With the data shown in Fig. 12 the final equations are, for the stable curves, eq. (60), $\nu = 2$:

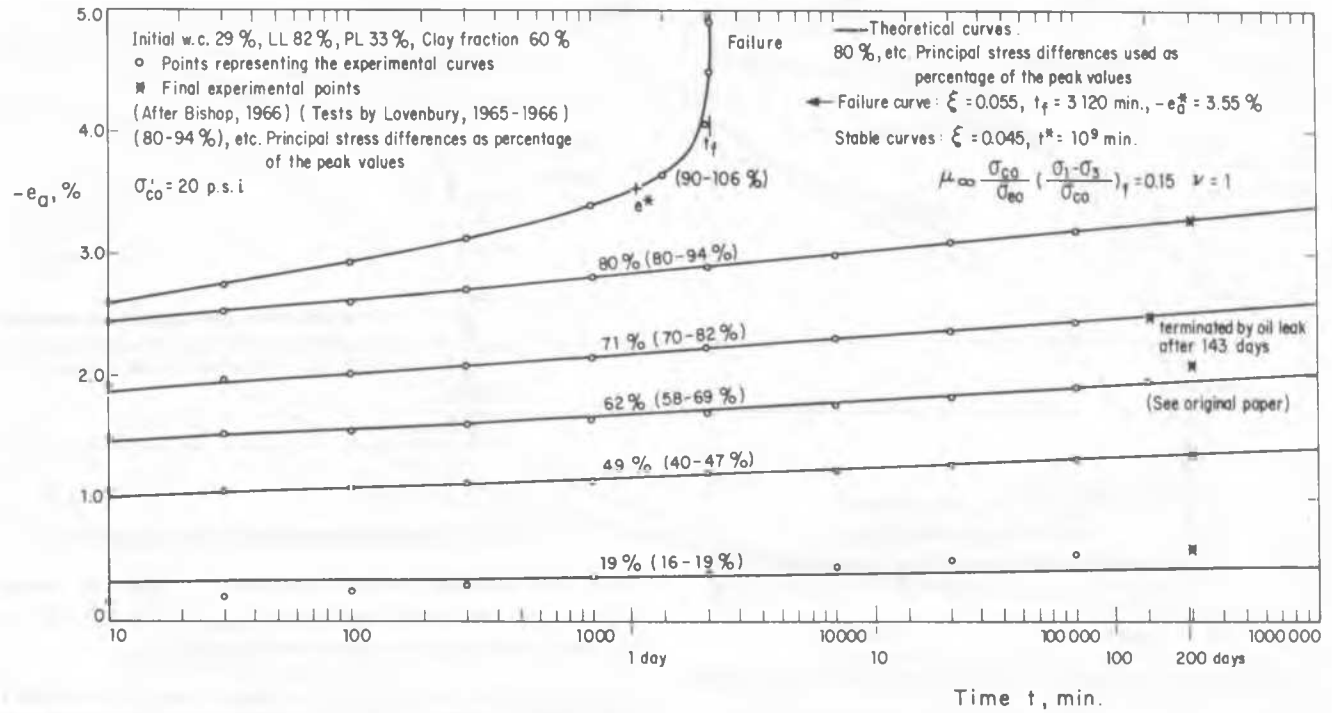

Fig. 7 Drained creep tests on undisturbed brown London clay from Hendon

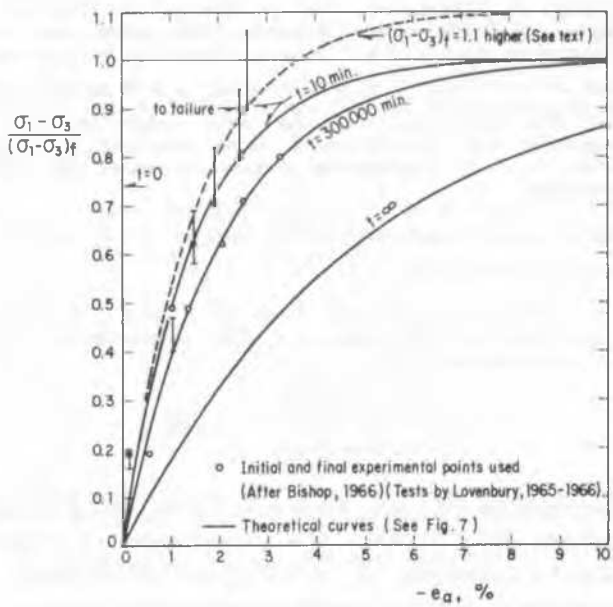

Fig. 8 Drained creep tests on undisturbed brown London clay from Hendon

$$-e_a,\ \% = 2.17\left[\frac{1}{1-\frac{D}{1.7}} - 1\right]\frac{1}{1+\left(\frac{t}{150{,}000}\right)^{-0.15}} \qquad (75)$$

and for the failure curves, eq. (22):

$$e_a,\ \% = e_a^* \left(\frac{t_f}{t} - 1\right)^{-\xi} \qquad (76)$$

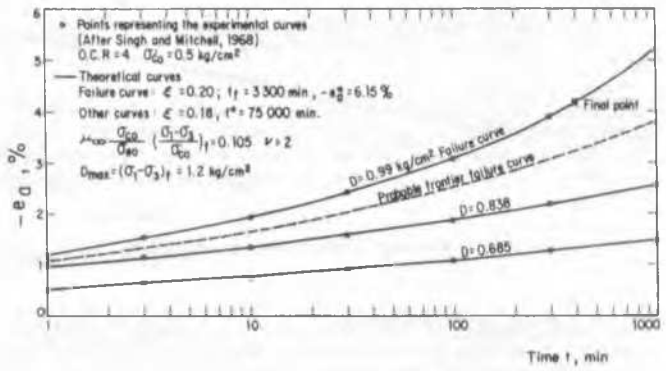

Fig. 9 Creep of overconsolidated undisturbed San Francisco bay mud.

where the specific values of ξ, e_a^* and t_f appear in Fig. 12 for each curve.

For this case it was found that the creep curve for D = 1.58 kg/cm^2 was a failure curve.

For the stable curves we can write

$$\xi = 0.15,\ t^* = 150{,}000 \text{ min},\ \frac{e_1}{e_\infty} = \frac{\mu_1}{\mu_\infty} = 0.14 \qquad (77)$$

For this case, the experimental points in Fig. 13 appear to indicate, again, higher strength at t = 1 min than at t =1,000 min.

Fig. 14 shows the application of eq. (41) to the failure data of Figs. 12 and 13. The failure data consist of only 2 points while 3 points are needed to define eq. (41). Fig. 14 shows the graphs of eq. (41) and the corresponding values of $(\sigma_1-\sigma_3)_{f\infty}$ for three values of ζ: 0.12, 0.18 and 0.30. The

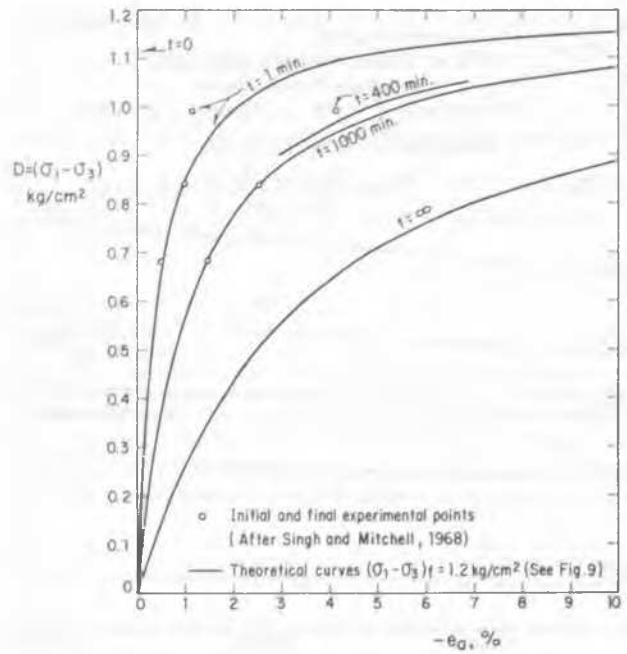

Fig. 10 Creep of overconsolidated undisturbed San Francisco bay mud

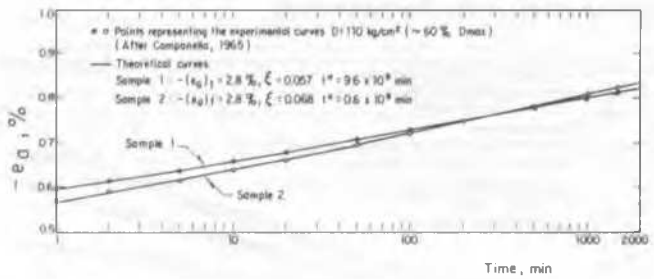

Fig. 11 Drained Creep tests on dry illite

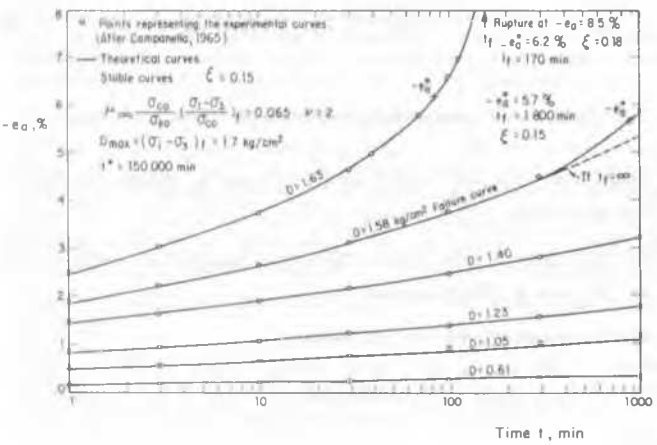

Fig. 12 Undrained creep of saturated remolded illite

values of t^*, eq. (42), are also shown. If, as an example, the values of ζ and ξ were equal, $\zeta=\xi$, the final equation would be, Eq. (42):

$$(\sigma_1-\sigma_3)_f, kg/cm^2 = 1.485\left[1+\left(\frac{t}{0.00041}\right)^{-0.18}\right] \qquad (78)$$

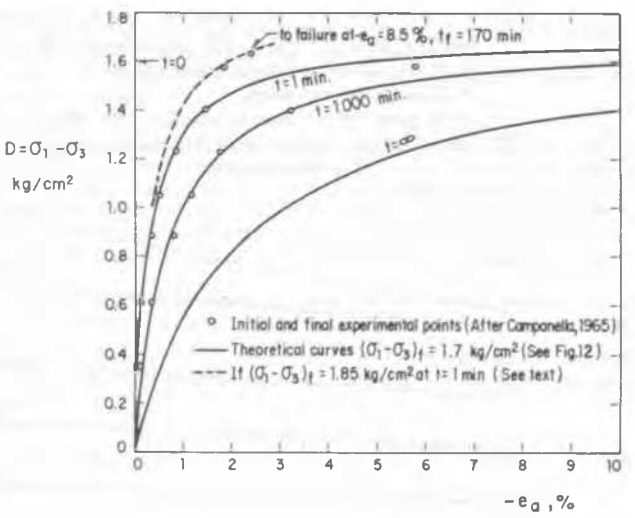

Fig. 13 Undrained creep of saturated remolded illite

and the strengths at t = 1 min and t = 1,000 min would be $(\sigma_1-\sigma_3)_{f1} = 1.85$ kg/cm^2 and $(\sigma_1-\sigma_3)_{f1000} = 1.59$ kg^2/cm^2, that is, 25% and 7% higher than at t = ∞, respectively.

At this point it is important to observe that at t = 1,000 min the stress - strain relation behaves as if the strength were somewhat higher than 1.7 kg/cm^2, Fig. 13, while the real strength is 1.59 kg/cm^2, Fig. 14, that is, the first is 7% higher than the second strength. This effect was first observed by Kondner (1963). However, from Fig. 14 it is found that at t = 1 min, if $\zeta = 0.18$, $(\sigma_1-\sigma_3)_f = 1.85$ kg/cm^2, value that fits very well with the upper points in Fig. 13, suggesting that the difference above mentioned is a time effect. Is it ?. Experimental evidence is needed for a final conclusion.

Some practical application of the variation of K_o with time, eq. (61), is as follows.

For Weald clay it was found $\phi = 21.8°$, $\gamma = 0.06$ (Juarez-Badillo, 1975) and $\mu = 0.10$ (Juarez-Badillo, 1988) and, therefore, eq. (61)

$$K_o = \frac{2.69 + \frac{0.10}{0.06} - 1}{2.69 + \frac{0.10}{0.06} + 1} = 0.63 \qquad (79)$$

This value is for $t = t_p$. For $t = 0$, $\phi = 90°$ and $\mu = 0$ and, therefore, $K_o = 0$. For $t = \infty$, if we consider the relation given for London clay $\mu_{10} = 0.30\ \mu_\infty$, eq. (69), we obtain for Weald clay $\mu_\infty = 0.33$ and assuming the same value of ϕ

$$K_{o\infty} = \frac{2.69 + \frac{0.33}{0.06} - 1}{2.69 + \frac{0.33}{0.06} + 1} = 0.78 \qquad (80)$$

and the progress of K_o with time would be given by eq. (61) with μ given by eq. (57) once the values of ξ and t^* for Weald clay are known.

Mesri and Castro (1987) have published some experimental data of $\frac{\Delta K_o}{\Delta \log t}$. In eq. (64), $\left.\frac{dK_o}{d \log t}\right]_{t=t^*}$ depends on ξ, $\frac{\mu_\infty}{\gamma}$ and

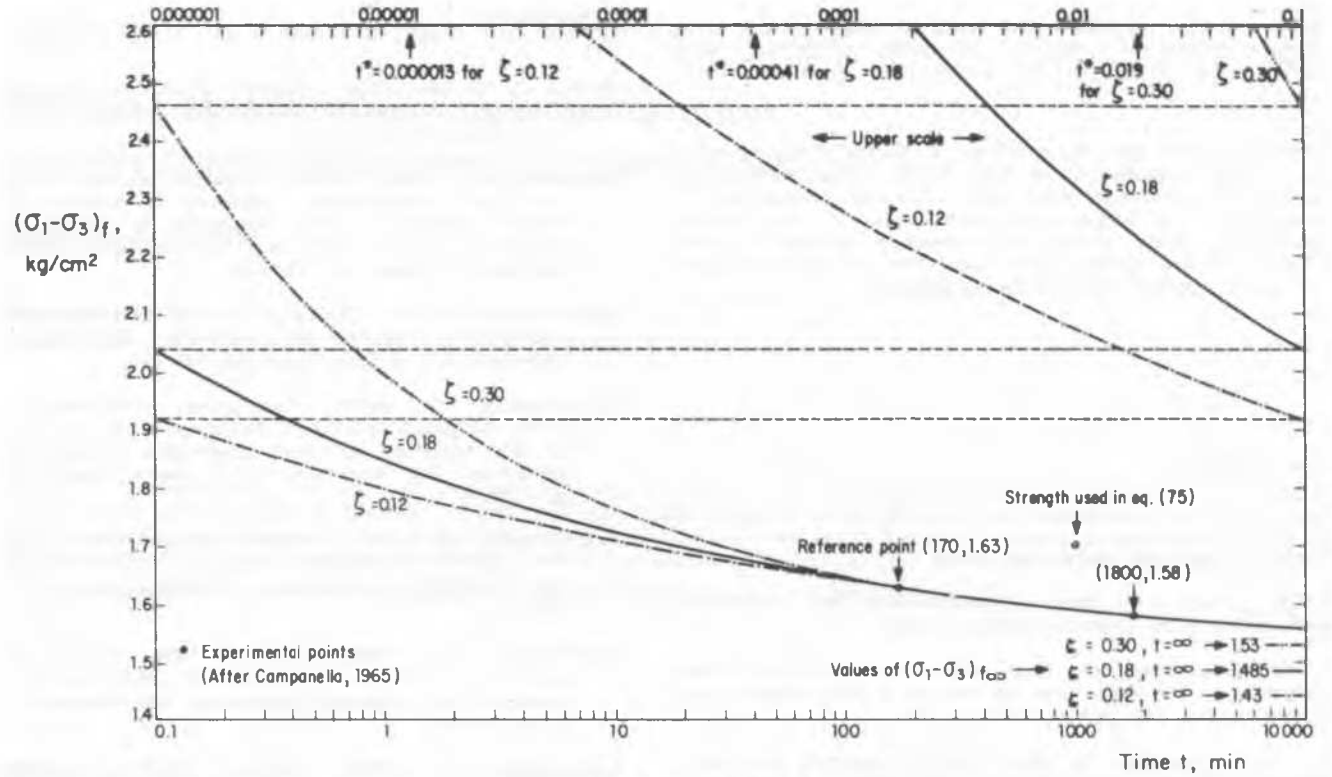

Fig. 14 Graphs of $(\sigma_1-\sigma_3)_f = (\sigma_1-\sigma_3)_{f\infty}\left[1+\left(\frac{1.63}{(\sigma_1-\sigma_3)_{f\infty}}-1\right)\left(\frac{t}{170}\right)^{-\zeta}\right]$ Undrained creep of saturated remolded illite

ϕ. For $\xi = 0.1$ the values of eq. (64) for different values of $\frac{\mu_\infty}{\gamma}$ and ϕ are

Table 1. Values of $\left.\frac{dK_o}{d\log t}\right]_{t=t^*}$ for $\xi = 0.1$

ϕ \ $\frac{\mu_\infty}{\gamma}$	2	5	10
20°	0.010	0.014	0.014
30°	0.014	0.019	0.018
40°	0.018	0.023	0.020

Taking into account that at $t < t^*$ these values may be of the order of 25% greater we have that for values of ξ from 0 to 0.3, the values of $\frac{dK_o}{d\log t}$ may be from 0 to 0.086.

The measured values for 5 clays are

Table 2. Values of measured $\frac{\Delta K_o}{\Delta \log t}$ (Mesri and Castro, 1987).

Soft clay	$\frac{\Delta K_o}{\Delta \log t}$
Bay Mud	0.025 - 0.065
Saint Alban	0.020
Broadback	0.045
Atchafalaya	0.038
Batiscan	0.070

The measured values reported in Table 2 are, therefore, within the range given by eq. (64). However, a final conclusion is to be reached by direct application of eqs. (61) and (57) to those clays.

FINAL COMMENTS

The main purpose of this paper is to present what are considered to be general relationships of deviatoric strains and strengths with time during the triaxial testing of geomaterials. Eqs. (14), (22) and (42) were found applying the principle of Natural Proportionality wich has been already applied to various physical phenomena (Juarez-Badillo, 1985b). The stress-strain equations (55) and (56) are considered still not to be general. They were included as a second step towards a general equation to be found in the future. Eqs. (55) and (56) were applied to Weald clay finding that eq. (55) is very good for drained tests, compression or extension, varying only the axial stress, varying only the radial stress or J_1 = cte. with $\mu = 0.10$ up to OCR = 24. Eq. (56) was found to be fairly good for undrained tests, for compression tests with $\mu = 0.04$ and extension tests with $\mu = 0.02$ up to OCR = 2. For higher OCR μ increased with the OCR in both types of tests, to a value of $\mu = 0.20$ for OCR = 24. This shows that eq. (56) needs great improvements.

To improve eqs. (14), (22) and (42) very good tests with great accuracy to include eq. (42) in eqs. (59) and (60) are needed as well as to dilucidate the difference between the real strength of soils at different times with the strength to be used in eqs. (59) and (60) if such a difference exist.

One important point is to find the factors that influence the values of the "fluidities", the volume fluidity δ (formerly

called volume viscosity), the shear fluidity ξ and the strength fluidity ζ. Mainly, do these properties vary with the type of triaxial test? And how do the scale affects them ?.

The author feels that the principle of Natural Proportionality may be applied succesfully to other physical phenomena such as to partially saturated soils and to dynamic properties of geomaterials. In respect to earthquakes, if the proper variable is found, which is necessarily related to the movement of the tectonic plates, eqs. (46) or (47) would give the time of the occurrence of the earthquakes.

CONCLUSIONS

The main conclusions may be as follows

1. The principle of Natural Proportionality has succesfully been applied to the creep phenomena in clays.

2. Simple equations have been found to describe the creep phenomena in the stable zone as well as in the unstable zone of geomaterials, eqs. (14) and (22).

3. A simple equation has been found to describe the shear strength of soils as function of time duration of deviatoric stress level in the unstable zone, eq. (42).

4. Simple equations describe the variation of K_o with time, eqs. (61) and (57).

5. "Instantaneous strains" at 1 or 10 min in triaxial tests are really a small part, of the order of 10 to 30%, of the final strains at $t = \infty$.

6. The shear fluidity ξ and the strength fluidity ζ, together with the volume fluidity δ, formerly introduced, appear to be fundamental properties of geomaterials.

7. Good experimental data, howewer, are needed to find the factors that influence the values of the fluidities mentioned.

8. The potentiality of the principle of Natural Proportionality to describe other physical phenomena is very promising.

ACKNOWLEDGEMENTS

The writer is indebted to the many researchers whose published experimental test results have been analyzed herein.

REFERENCES

Bishop, A. W.(1966). The strength of soils as engineering materials. 6th Rankine Lecture, Geotechnique, Vol. 12, No. 2, june 1966, pp. 91-130.

Campanella, R.G. (1965). "Effect of temperature and stress on the time - deformation behaviour in saturated clay. Thesis presented to the University of California at Berkeley in partial fulfillment of the requirements for the degree of Doctor of Philosophy.

Juárez-Badillo, E.(1974). Theory of natural deformation. First Australian conference on engineering materials, the University of New South Wales, pp. 441-465.

Juárez-Badillo, E. (1975). Constitutive relationships for soils. Symposium on recent developments in the analysis of soil behaviour and their application to geotechnical structures, the University of New South Wales, Sidney, pp. 231-257.

Juárez-Badillo, E. (1981). General compressibility equation for soils. X International Conference on soil mechanics and foundation engineering, Stockholm, Vol. 1, pp. 171-178.

Juárez-Badillo, E. (1985a). General time volume change equation for soils. XI International Conference on soil mechanics and foundation engineering, San Francisco, Vol. 2, pp. 519-530.

Juárez-Badillo, E. (1985b). General volumetric constitutive equation for geomaterials. Constitutive laws of soils, Report of ISSMFE Subcommittee on constitutive laws of soils and proceedings of discussion session 1A XI ICSMFE, Japan, pp. 131-135.

Juarez-Badillo, E. (1988). Basic stress-strain equation for soils. Internal report, DEPFI, UNAM, Mexico.

Juarez-Badillo, E. (1990). General stress-strain-time equation for soils. Internal report, DEPFI, UNAM, Mexico.

Juarez-Badillo, E. and Rico-Rodriguez A. (1975). Mecánica de Suelos, Tomo 1, Fundamentos de Mecánica de Suelos, Capítulo XIII, Limusa, Mexico.

Kondner, R. L. 1963. Hyperbolic stress- strain response: cohesive soils. Journal of the Soil Mechanics and Foundation Division, ASCE, Vol. 89, No. SM-1, february 1963, pp. 115-143.

Mesri G. and Castro A.(1987). $C\alpha/Cc$ concept and K_o during secondary compression. Journal of Geotechnical Engineering, ASCE Vol. 113, No. 3, march 1987, pp. 230-247.

Singh A. and Mitchell J.K. (1968). General stress-strain-time function for soils. Journal of the Soil Mechanics and Foundation Division, ASCE, Vol. 94, No. SMI, January 1968, pp. 21-46.